Performance Analysis of Hydrogen Aircraft using Optimal Control

Inderawan, A.P.S.; Hoogreef, M.F.M.; Nie, Yuanbo

DOI
10.13009/EUCASS2025-240

Publication date
2025

Document Version
Final published version

Citation (APA)
Inderawan, A. P. S., Hoogreef, M. F. M., & Nie, Y. (2025). *Performance Analysis of Hydrogen Aircraft using Optimal Control*. Paper presented at 11th European conference for aeronautics and space sciences, Rome, Italy. https://doi.org/10.13009/EUCASS2025-240

DOI: 10.13009/EUCASS2025-240
11TH EUROPEAN CONFERENCE FOR AERONAUTICS AND SPACE SCIENCES (EUCASS)

Performance Analysis of Hydrogen Aircraft using Optimal Control

*Ardya Inderawan**†, Maurice Hoogreef* and Yuanbo Nie‡*
** Delft University of Technology*
Kluyverweg 1, 2629 HS Delft, The Netherlands
‡ The University of Sheffield
Western Bank, Sheffield S10 2TN, United Kingdom
a.p.s.inderawan@tudelft.nl – m.f.m.hoogreef@tudelft.nl – y.nie@sheffield.ac.uk
† Corresponding Author

Abstract
Solid oxide fuel cell-gas turbine (SOFC-GT) propulsion system using hydrogen fuel, is a promising option to minimize climate impact of aviation. However, a slower response time is one possible outcomes of utilizing SOFC-GT, which affects aircraft performance, particularly in transient scenarios such as go-arounds. The effect of engine response times on the flight trajectory of a go-around manoeuvre are investigated numerically by solving an optimal control problem that minimizes the time needed to perform the manoeuvre. Results shows a 111% more altitude loss by operating an engine with a 20 seconds response time compared to a 5 seconds engine.

1. Introduction

In the conceptual phase of aircraft design, performance is commonly evaluated using steady-state equations such as the Breguet range equation. Yet, with a growing focus on climate-friendly development goals, novel propulsion technologies are coming into view, which require a modification to this equation [1].

The HYLENA project, for instance, is investigating a novel engine architecture that merges a solid oxide fuel cell (SOFC) with a gas turbine (GT), to reduce aviation's climate impact through high efficiency and carbon neutrality using hydrogen fuel [2]. These technologies, although promising for environmental benefits, could have a slower response times due to the thermal inertia of the SOFC which has an operating range of 600 – 1000 degrees C.

A study on land-based applications showed that a ramp-down of 48.4% can be achieved in 10 seconds using a novel control strategy [4]. However, 10 seconds is still not enough for aircraft applications, as the regulation for aircraft engines requires a demonstrated capability on the test bed, ramping up from 15% to 95% rated power or thrust in under 5 seconds [5]. The effect of this response time on the transient performance of the aircraft, cannot be captured using commonly used steady-state equations. With various options of propulsion system architectures, it is important to study the response time for novel architectures and its impact on the overall aircraft design and performance.

To investigate the effect of engine response time, optimal control, typically applied in trajectory optimization research, is used to assess the transient performance of aircraft [6]. Instead of the steady-state approximation, the differential flight equations of motion are solved directly, giving information on the state of the aircraft during a certain point in time. Utilizing ICLOCS[1]to solve the optimal control problem, the optimum trajectory and control history for the aircraft to move from the initial to the final state can be found for a given objective function, such as minimizing the time required for the climb [7].

This research investigates the effect of introducing a lag between throttle input and thrust response, to the optimum flight trajectory and control history. One example of the optimal control problem to be investigated is a time minimum go-around manoeuvre, which provides a realistic assessment of aircraft operational performance in transient operation with new propulsion systems. This point of view complements the research of Buell and Leondes [8], who has investigated the optimal control solution for minimum height loss during the go-around manoeuvre.

In this article, it is initially hypothesized that accounting for engine response time will significantly affect the flight trajectory, especially in emergency scenarios where quick thrust adjustments are crucial. This hypothesis is tested by numerically solving the flight equations of motion in the longitudinal axis during a one engine inoperative go-

[1] Imperial College London Optimal Control Software, accessible from http://www.ee.ic.ac.uk/ICLOCS/default.htm

DOI: 10.13009/EUCASS2025-240

around manoeuvre as specified in Certification Specification (CS) 25.101(g) [9] while using an optimum control strategy.

The findings show that there is a correlation between engine response time to altitude loss, which translates to decision height required to operate the aircraft, as well as different control input to perform a go-around for different engine responses. These results aids in assessing the operational risks and benefits of aircraft fitted with new propulsion technologies, as well as identifying critical points required to size the engine during the conceptual phase of aircraft design.

This article consists of two main sections, followed by a concluding section for to summarise the findings and future work. Section 2 describes the mathematical model for the go-around problem with the assumptions and values used in the calculations. Then, Section 3 presents the results on a validation case, as well as results from different engine response times on the trajectory of go-around manoeuvre.

2. Model and Methodology

2.1 Aircraft Model

In this work, a turboprop aircraft (ATR 72) is modelled as a point mass and the movement is limited to longitudinal motions (x-z axes). The forces acting on the aircraft are depicted below.

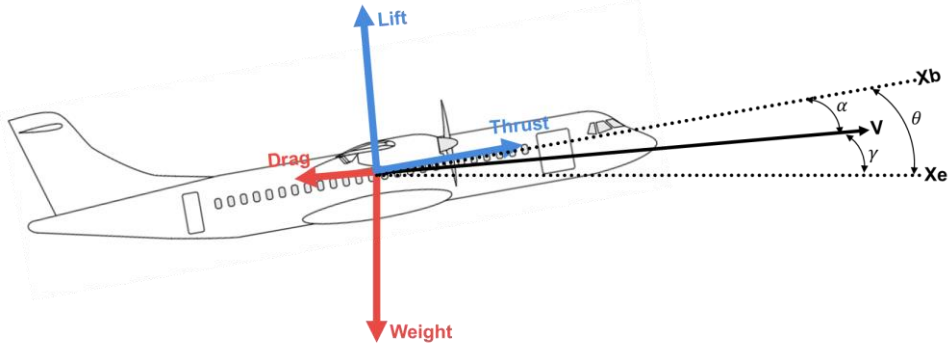

Figure 1: Aircraft free-body diagram

In this model, it is assumed that there is no engine setting angle so that the thrust force is in-line with the body axis $\boldsymbol{X_b}$. Lift is perpendicular to drag and both are acting on the wind axis. Assuming no wind condition, the airspeed is the relative movement of air against the moving aircraft, with the wind axis the same as aircraft velocity $\boldsymbol{V}$ along the flight path. The pitch angle of the aircraft $\boldsymbol{\theta}$ is the angle between body axis and earth axis $\boldsymbol{X_e}$, which is a sum of the angle between body axis and wind axis, angle of attack $\boldsymbol{\alpha}$, and the angle between wind axis and earth axis, flight path angle $\boldsymbol{\gamma}$.

Aircraft states that are of interest in this research are mass $\boldsymbol{m}$, airspeed $\boldsymbol{V}$, and flight path angle $\boldsymbol{\gamma}$, which are governed by the following simplified flight equations of motion.

$$\theta = \alpha + \gamma \tag{1}$$

$$m\frac{dV}{dt} = T\cos\alpha - D - mg\sin\gamma \tag{2}$$

$$mV\frac{d\gamma}{dt} = L + T\sin\alpha - D - mg\cos\gamma \tag{3}$$

$$\frac{dm}{dt} = -\frac{T}{g \cdot I_{sp}} \tag{4}$$

$$\frac{dh}{dt} = V\sin\gamma \tag{5}$$

$$\frac{dx}{dt} = V\cos\gamma \tag{6}$$

DOI: 10.13009/EUCASS2025-240

$$\frac{d\theta}{dt} = \dot{\theta} \tag{7}$$

$$\frac{d\dot{\theta}}{dt} = \ddot{\theta} \tag{8}$$

Where $\boldsymbol{T}$, $\boldsymbol{L}$, and $\boldsymbol{D}$ is respectively thrust, lift, and drag forces. The gravitational acceleration $\boldsymbol{g}$ is assumed to not vary with altitude at a value of 9.81 m s^{-2}. $\boldsymbol{I_{sp}}$ is specific impulse as a characteristic of the engine being modelled, illustrating how much fuel the engine consumes to provide a certain amount of thrust. For turboprop aircraft, Brake Specific Fuel Consumption (BSFC) is more commonly used metric and inversely proportional, $I_{sp} = 1/(g \cdot BSFC)$. $\boldsymbol{h}$ is position of the aircraft in vertical axis, and $\boldsymbol{x}$ is the position in the horizontal axis.

In a more detailed manner, lift is a function of air density $\boldsymbol{\rho}$, wing area $\boldsymbol{S}$, and wing lift coefficient $\boldsymbol{C_L}$, which is assumed to be in the linear region and is a function of angle of attack $\boldsymbol{\alpha}$.

$$L = 0.5\,\rho\,V^2 S\,C_L \tag{9}$$

$$C_L = C_{L_0} + C_{L_\alpha}\alpha \tag{10}$$

Where $\boldsymbol{C_{L_0}}$ is the lift coefficient of the wing at zero angle of attack, and $\boldsymbol{C_{L_\alpha}}$ is wing lift curve slope, computed using DATCOM[2] method [10].

$$\frac{dC_L}{d\alpha} = C_{L_\alpha} = \frac{2\pi\,AR}{2 + \sqrt{4 + (\frac{AR\,\beta}{\kappa})^2(1 + \frac{tan^2\,\Lambda_{0.5C}}{\beta^2})}} \tag{11}$$

In this equation, $\boldsymbol{AR}$ is the aspect ratio of the wing, in this case is assumed to be 12. $\boldsymbol{\Lambda_{0.5C}}$ is the sweep angle of the wing, measured from half chord length. $\boldsymbol{\beta}$ is Prandtl-Glauert compressibility correction factor $\beta = [(1 - M_\infty^2)]^{\frac{1}{2}}$, with $\boldsymbol{M_\infty}$ as the Mach number of the free stream, related to the true airspeed $\boldsymbol{V}$ and speed of sound at a given altitude $\boldsymbol{a}$. $\boldsymbol{\kappa}$ is the ratio of the lift curve slope of the wing airfoil to the theoretical lift curve slope of 2π rad^{-1}. In this study, the wing is assumed to be using a NACA 43013 airfoil. Evaluating the lift curve slope of the airfoil using XFOIL[3] with a Reynolds number of 10^7 and Mach number of 0.18, representative of approach speed, results in a $\boldsymbol{\kappa}$ value of 0.94. [1]

While the lift curve slope of the airfoil is 6% lower than the theoretical value, the choice of airfoil also affects the maximum attainable airfoil lift coefficient $\boldsymbol{C_{l_{max}}}$, therefore affecting maximum wing lift coefficient $\boldsymbol{C_{L_{max}}}$, and the angle of attack at which a stall occurs $\boldsymbol{\alpha_s}$, both in the clean configuration and flap extended configuration. Using XFOIL and DATCOM method described in [10], it is found that $\boldsymbol{C_{l_{MAX}}}$ of the airfoil is 1.70, $\boldsymbol{C_{L_{MAX}}}$ of the wing is 1.52, and stalls at $\boldsymbol{\alpha_s}$ of 13.47 degrees.

As the scope of this study is focused on go-around, the aircraft configuration of interest will be the landing configuration, where the landing gear and flaps are deployed. The wing is assumed to use a fowler flap as illustrated in Figure 2.

[2] USAF Digital Datcom, accessible from https://www.pdas.com/datcom.html
[3] XFOIL version 6.99, accessible from web.mit.edu/drela/Public/web/xfoil/

DOI: 10.13009/EUCASS2025-240

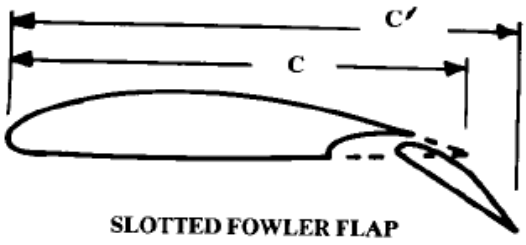

Figure 2: Fowler flap [2]

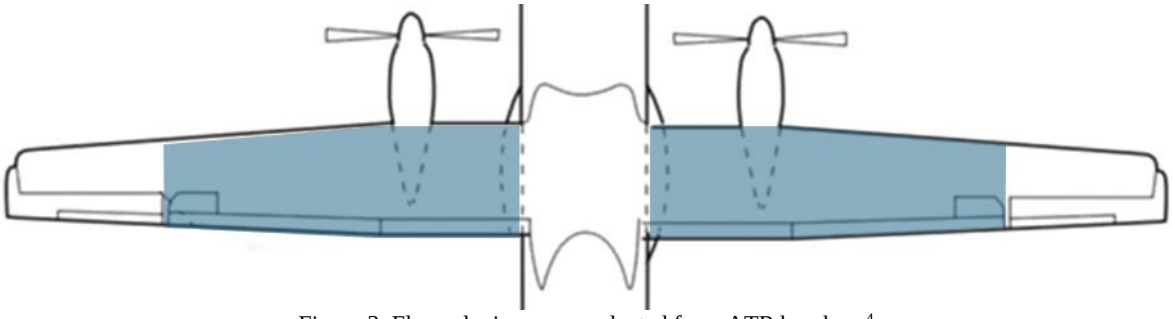

Figure 3: Flapped wing area – adapted from ATR brochure[4]

Deployment of flaps increases the lift curve slope and maximum wing lift coefficient, as well as reduces the stall angle of attack. These values are computed using method described in Appendix G-2 of [12]. In this study, the fraction of wing area covered by flaps as shown in Figure 3 is measured to be 0.67 using OpenVSP[5] and the fraction of flap chord to wing chord is 0.3.

The drag of the aircraft is calculated using standard drag equation as follows.

$$D = 0.5\,\rho\,V^2 S\,C_D \tag{12}$$

The aircraft is assumed to be capable of cruising at a maximum cruise speed of 275 knots at an altitude of 27 000 feet with 97% of the maximum take-off weight based on [13]. During cruise, $\boldsymbol{T = D}$ and $\boldsymbol{L = W}$, therefore by using a thrust value, the drag coefficient $\boldsymbol{C_D}$ can be calculated. The total thrust of the turboprop engine considering both thrust generated from the propeller as well as the jet exhaust is approximated in the following equation.

$$T = \frac{1\,000\,P\,\eta_{prop}}{V} + \left(\frac{P}{2} + 96.1\right) \tag{13}$$

$$P = P_{SL}\,\sigma \tag{14}$$

Where the units of engine power $\boldsymbol{P}$ is in kW, $\boldsymbol{V}$ in m s^{-1}, $\boldsymbol{T}$ in N, and the propeller efficiency $\boldsymbol{\eta_{prop}}$ is assumed to be constant at 0.8. The first term accounts for the thrust generated by the propeller, and the second term of the thrust equation is the residual thrust generated by the jet exhaust as a linear regression of residual thrust data based on [3].

The engine is assumed to operate in the maximum sea level continuous power $\boldsymbol{P_{SL}}$ of 1 864 kW. With the engine power available at cruise altitude corrected with the air density ratio $\boldsymbol{\sigma}$, the $\boldsymbol{C_D}$ is found to be 0.0285. The lift coefficient $\boldsymbol{C_L}$ at cruise condition is calculated to be 0.4924.

$$C_D = C_{D_0} + k\,C_L^2 \tag{15}$$

[4] At the time of writing, accessible from https://www.atr-aircraft.com/wp-content/uploads/2020/07/72-500.pdf
[5] OpenVSP version 3.41.1, accessible from https://openvsp.org/download_old.php

DOI: 10.13009/EUCASS2025-240

$$k = \frac{1}{\pi\, AR\, e_0} \tag{16}$$

Using the quadratic approximation of drag polar, aspect ratio $\boldsymbol{AR}$ value of 12, and Oswald's efficiency factor $\boldsymbol{e_0}$ value of 0.8, the following drag polar equation is constructed.

$$C_D = \left(0.0205 + \Delta C_{D_0}\right) + 0.0265\, \frac{C_L^2}{e_0 + \Delta e_0} \tag{17}$$

In this equation, landing gear and flap deployment also affects the drag coefficient of the aircraft by increasing the zero-lift drag coefficient $\boldsymbol{C_{D_0}}$ and Oswald's efficiency factor $\boldsymbol{e_0}$. The increment in $\boldsymbol{\Delta C_{D_0}}$ and $\boldsymbol{\Delta e_0}$ due to flap and landing gear extension compared to clean configuration is assumed to be 0.037 and 0.015.

2.2 Engine Response Model

In a go-around situation, it is considered valid to assume a step input to the maximum allowable thrust by the pilot. However, the actual thrust delivered by the engine depends on how fast the engine responses. An exponential decay function is used to simulate different response times of the engines based on [8].

$$P(t) = P_{max} + \left[P(t_0) - P_{max}\right] * e^{-(t-\delta)/\tau} \tag{18}$$

Compared to the original equation, a modification is made to use power instead of thrust as the variable and addition of delay component, to better reflect the operation of a turboprop aircraft. As the turboprop aircraft still uses a gas turbine, the exponential decay based on engine time constant $\boldsymbol{\tau}$ still holds. However, compared to turbofan aircraft, a turboprop with a constant speed propeller is able to adjust the propeller blade pitch to convert the power from the engine into thrust. The adjustment of the blade pitch is not instantaneous, and this is covered with an addition of a delay $\boldsymbol{\delta}$, which can include the delay due to the movement of propeller governor. These delays are illustrated in Figure 4.

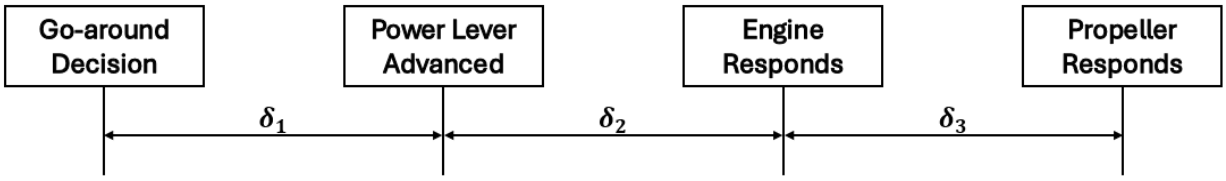

Figure 4: Delays between actions in go-around

In this equation, $\boldsymbol{P_{max}}$ is calculated from maximum available takeoff/go-around power at a given altitude, $\boldsymbol{P(t_0)}$ is the power at the start of the manoeuvre – assumed idle or zero – , $\boldsymbol{\delta} = \delta_1 + \delta_2 + \delta_3$ is the total delay in seconds between the go-around decision and the thrust response of the engine, and $\boldsymbol{\tau}$ is the engine time constant.

In this research, engine response time is defined as the time for the engine to accelerate from 15% to 95% rated power, as defined by Certification Specifications for Engines (CS-E) 745 for gas turbines [5]. The value of $\boldsymbol{\tau}$ that that meets the CS-E 745 engine acceleration requirements in 5 seconds is calculated to be 1.7530. This value varies linearly with engine response time. In other words, a slower engine that meets CS-E requirements in 20 seconds has a $\boldsymbol{\tau}$ value of 7.060, and a faster engine that meets CS-E requirements in 1 second has a $\boldsymbol{\tau}$ value of 0.3530. An illustration of how the engine responds over time is depicted in Figure 5.

DOI: 10.13009/EUCASS2025-240

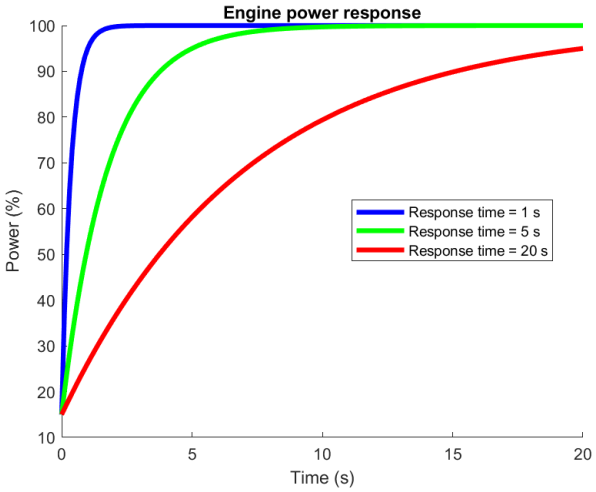

Figure 5: Different engine responses

2.3 Go-around Optimal Control Problem

The approach in solving the go-around problem used in this research is by seeking an optimal control strategy that results in the minimum time to reach the required climb gradient as specified in CS 25.119 for all engine operating, and CS 25.121(d) for one engine inoperative condition [9]. To ensure that the solution is executable in real operation by crews of average skill, another cost function to minimise the amount of control input is added. As the control input can be positive or negative, the cost function of control input is squared.

The total cost function is therefore to minimise the sum of time needed to complete the manoeuvre $\boldsymbol{t_f}$ and area under the curve of control input squared.

$$\min_{\boldsymbol{X},\boldsymbol{U},t_f} t_f + \int_{t_0}^{t_f} \boldsymbol{U}^2 \, dt \tag{19}$$

In this optimal control problem, $\boldsymbol{X}$ is the state vector of the aircraft (altitude, mass, airspeed, flight path angle, horizontal position, pitch, and pitch rate), and $\boldsymbol{U}$ is the control input subject to previously mentioned flight equations of motion as the governing dynamics.

In operation, pilot action of pulling or pushing on the control stick changes the elevator deflection angle, and thereby changing the force on the tail. This change of force then creates an angular acceleration around the centre of gravity in the pitch axis. However, the relation between the deflection of the elevator angle and the force on the tail is not entirely linear, as it is essentially changing the camber of an airfoil. To simplify, pitch acceleration is chosen as the control input.

Based on the chosen aircraft, the bounds on the states and variables are as follows.

$$15\,000 \leq m \leq 22\,350 \text{ [kg]} \tag{20}$$

$$91.1 \leq V \leq 275 \text{ [knots]} \tag{21}$$

$$\alpha \leq 13.47 \text{ [degrees]} \tag{22}$$

$$\theta \leq 20 \text{ [degrees]} \tag{23}$$

$$-4 \leq \dot{\theta} \leq 4 \text{ [degrees/s]} \tag{24}$$

The pitch angle $\boldsymbol{\theta}$ and pitch rate $\dot{\boldsymbol{\theta}}$ is limited based on the criteria to mitigate the risks of somatogravic illusions during the go-around based on Acceptable Means of Compliance (AMC) 25.143(b)(4) of [9]. The angle of attack is limited based on the angle at maximum lift coefficient $\boldsymbol{C_{L_{max}}}$ with flap deflected at 35 degrees, which is calculated using

DOI: 10.13009/EUCASS2025-240

method described in Appendix G-2 of [2]. The lower limit of $\boldsymbol{V}$ is the reference stall speed $\boldsymbol{V_{SR}}$, which is calculated using maximum landing weight $\boldsymbol{MLW}$ and maximum lift coefficient with flaps deployed $\boldsymbol{C_{L_{max,flapped}}}$. The upper limit of $\boldsymbol{V}$ is based on the maximum cruise speed of ATR 72 based on[13]. The mass of the aircraft is limited by the operating empty weight $\boldsymbol{OEW}$ and maximum take-off weight $\boldsymbol{MTOW}$.

For aircraft with all engines operating, the go-around is achieved when the aircraft achieved a state of 3.2% climb gradient $\boldsymbol{CGR_f}$ at an altitude $\boldsymbol{h_f}$ equal to the decision height $\boldsymbol{h_0}$ or equal to the span of the wing, with a speed $\boldsymbol{V_f}$ that is not more than 1.4 $\boldsymbol{V_{SR}}$. The terminal condition can be described as follows.

$$CGR_f = 3.2\% \tag{25}$$

$$V_f \leq 1.4\, V_{SR} \tag{26}$$

$$h_f = h_0 \tag{27}$$

2.4 OEI Go-around Criteria

The One Engine Inoperative (OEI) go-around problem is formulated according to AMC 25.101(g) Go-around, shown in Figure 6.

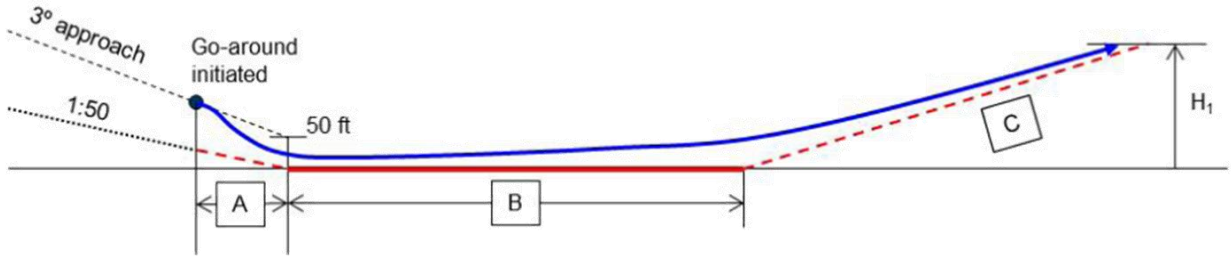

Figure 6: Go-around assessment [3]

The aircraft initially approaches the runway following a 3-degree glideslope, in a specified approach speed not higher than reference speed +5 knots, with mass assumed to be at the maximum landing mass. At a specified decision height, the go-around is initiated, and pilot demands maximum thrust from the engine and starts to apply a certain pitch strategy to achieve a successful go-around.

The go-around is achieved successfully when the aircraft achieve a steady climb gradient $\boldsymbol{CGR_f}$ of 2.1% for a two-engine aircraft, at a climb speed of no higher than 1.4 times the stall speed of the aircraft in approach configuration, while remaining above the red lines in Figure 6. Line segment A is a straight line in a 2% slope from the edge of the runway, segment B is a straight line defined as 40 times the approach speed in m s^{-1}, and segment C is a straight line from the end of segment B with 2.1% gradient for two-engine aircraft. $\boldsymbol{H_1}$ is a height above runway elevation, out of ground effect (1 times wingspan) that needs to be achieved by the aircraft, and no less than the decision height. Therefore, the termination criteria for the optimal control problem becomes as the following.

$$CGR_f = 2.1\% \tag{28}$$

$$h_f \geq H_1 \tag{29}$$

In the initial condition where go-around is decided, the value of stall reference speed $\boldsymbol{V_{SR}}$ is calculated at maximum landing weight $\boldsymbol{MLW}$ of 22 350 kg and maximum lift coefficient $\boldsymbol{C_{L_{max}}}$ of 2.473 obtained through XFOIL and DATCOM method assuming a flap deflection of 35 degrees. Reference speed $\boldsymbol{V_{REF}}$ is 1.23 times $\boldsymbol{V_{SR}}$ and calculated to be 91.1 knots and therefore the initial approach speed $\boldsymbol{V_0}$ used to proof compliance to go-around regulation is 96.1 knots.

In the beginning of the manoeuvre, the aircraft approached runway following a 3 degrees glideslope, which means a flight path angle $\boldsymbol{\gamma_0}$ of -3 degrees.

DOI: 10.13009/EUCASS2025-240

The decision height is assumed to be 200 ft, corresponding to the limit of CAT I approach. At this decision height, if required visual reference has been established, a pilot may continue the approach to land on the runway.

The initial pitch angle of the aircraft $\boldsymbol{\theta_0}$ is chosen based on the speed and weight, taking into account wing incidence angle $\boldsymbol{i_w}$ which is assumed to be 2 degrees based on data of ATR 42 aircraft, which the ATR 72 is developed from [13].

The result trajectory is checked against AMC 25.101(g), making sure that the trajectory does not cross the red limit lines.

3. Results and Discussions

To ensure the validity of the proposed methodology, a comparison to a real flight data is first performed, before applying the method for a hypothetical hydrogen aircraft. The source of this data is an aircraft incident report where an ATR 72 aircraft performed a go-around below the decision height due to the runway visual range being less than required [14].

3.1 Validation Case

In this validation case, the initial conditions are based on the contents of an incident report of LY-JUP aircraft on 12 August 2024 [14].

As mentioned in the report [14], the power levers were advanced to full power when the aircraft was at a radio altitude of 70 ft above ground level and 116 Knots Indicated Airspeed (KIAS) (point D), at 08:43:47 GMT. Therefore, the initial altitude is 70 ft above the runway elevation of 336 ft.

Assuming airspeed sensors are properly calibrated, the indicated airspeed is assumed the same as the calibrated airspeed. This airspeed is then converted to true airspeed, resulting in a value of 116.7 knots as the initial airspeed.

The aircraft at the time was flying with 5 crew members and 52 passengers, the exact payload mass is unknown, but it is scaled against the 7 500 kg maximum payload mass of the aircraft based on [13], resulting in a payload mass of 5 417 kg. The OEW is 13 311 kg based on [13].

As the aircraft ultimately diverted to Southampton airport, it is also assumed that at the time of the go-around, the aircraft still has enough fuel to perform a 45-minute flight with an assumed BSFC of 330 kg/kW/h, resulting in a fuel weight of 922.5 kg. Therefore, the initial mass of the aircraft during the go-around manoeuvre is assumed to be 19 650 kg.
The initial pitch angle is -0.6 degrees based on the FDR data, and an initial flight path angle of -3 degrees is assumed, representing the glideslope for a standard approach. This assumption is used instead of calculating the flight path angle from the FDR data as there is no angle of attack data available, and it is likely that the FDR data has a 1 Hz sampling rate and calculating the vertical speed from this data yields unwanted fluctuations.

As the aircraft is trimmed to fly in this glideslope, it is also assumed that there is no pitch acceleration in the initial condition.

During the approach, the power of the engine is set to be at the minimum flight idle, typically around 3% of the maximum power. FDR data shows a value of 3.2% is used by the aircraft. The engine time constant is assumed to be 1.7530 s, as the engine is certified to meet CS-E 745. The delay of engine response is adjusted to better fit the engine torque data with a value of 2.75 seconds. This value includes the movement of power lever angle from idle to go-around setting, which is reasonably expected in service and aligned with AMC 25.101(g) that this delay should not be less than one second.

The exit criteria of this go-around, as it is all engine operating condition, is 3.2% climb gradient. This condition must be achieved with a speed that is less than 1.4 $\boldsymbol{V_{SR}}$, meaning less than 201 knots. The altitude at which this condition must be achieved is equal to the span of the aircraft, as the go-around is initiated at an altitude below the span length, which is 27.05 meters or 89 ft.

DOI: 10.13009/EUCASS2025-240

The results from solving the optimal control problem are depicted in the next figures, where the results are plotted over the data trace from the flight data recorder from Point D of Figure 7 [14].

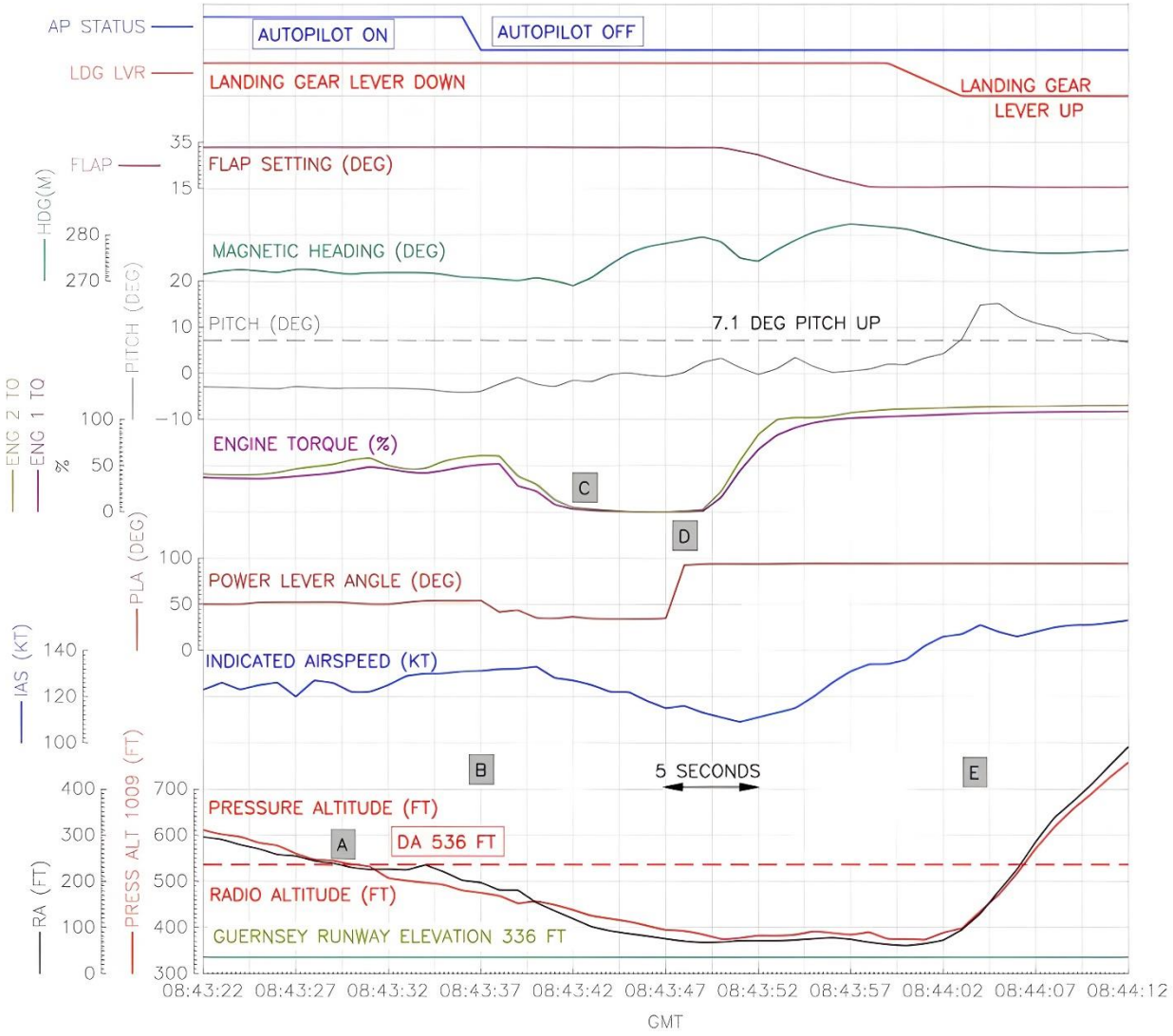

Figure 7: Flight Data Recorder (FDR) data of LY-JUP flight on 12 August 2024[14]

DOI: 10.13009/EUCASS2025-240

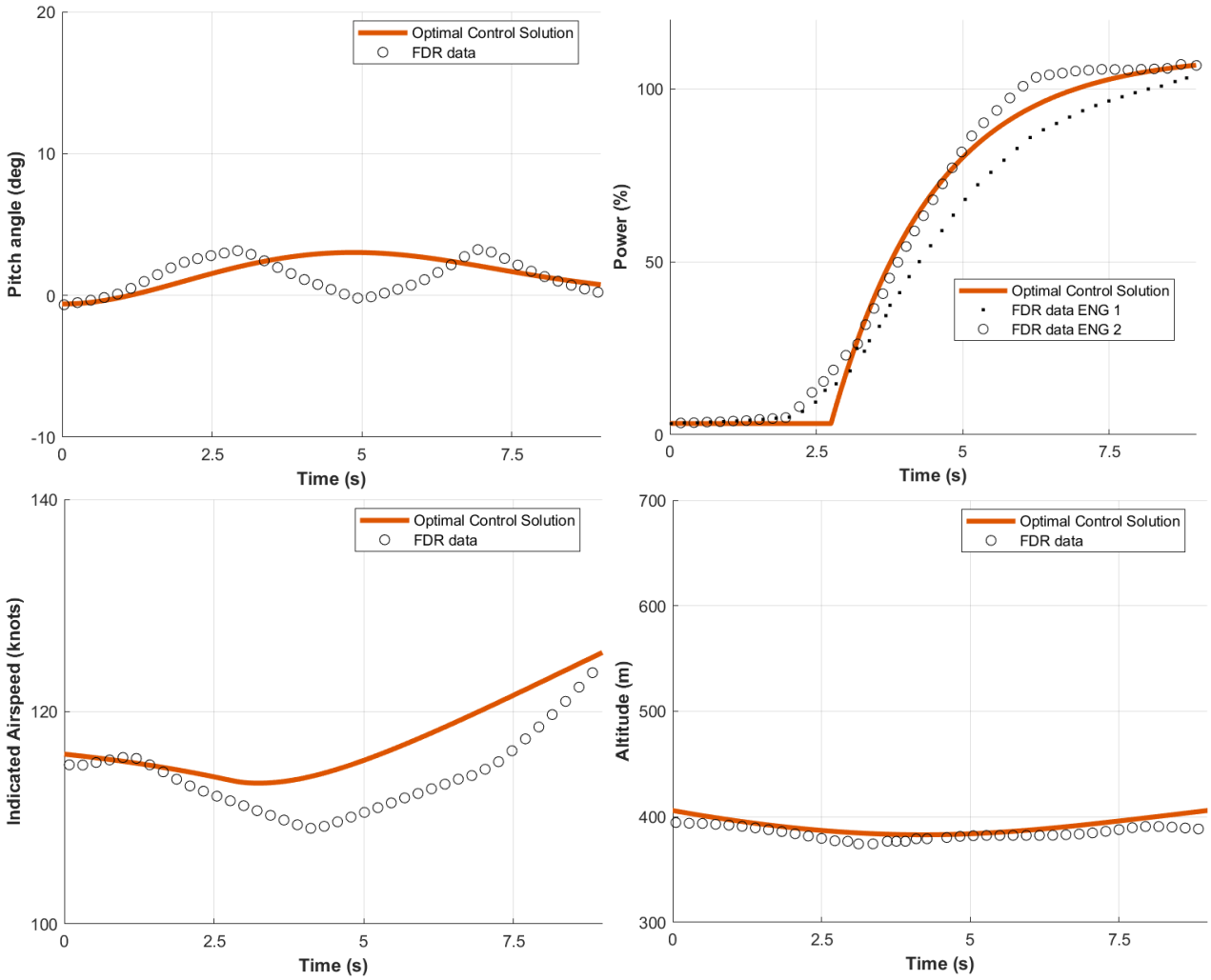

Figure 8: Superimposed results: a) Pitch angle, b) Torque, c) Airspeed, d) Altitude

As shown in the superimposed Figure 8, the optimal control method with previously mentioned cost function (19) is showing similar trend with the achievable go-around manoeuvre in a real flight situation by flight crews.

Looking at the pitch angle graph on Figure 8a, it can be seen that the optimal control solution does not require a sharp increase in pitch angle, even without imposing a pitch acceleration limits. The maximum pitch angle achieved is also below the 7.1-degree limit, far below the 20 degrees boundary set in the previous methodology explanation, and aligned closely with the maximum pitch angle achieved by the flight crew inputs.

The most striking difference is that the flight crew increased the pitch angle earlier than optimal control solution. This results in a slightly larger dip on the indicated airspeed, as the engine does not produce enough torque to generate the required thrust yet.

The simplistic model of engine power response behaves quite similarly in the upper range, but differently in the lower range of power. It can be seen in the real data shown on Figure 8b that less than 2.5 seconds after Point D, the engine already start to respond to the power demand, but with a shallower slope. This shallow slope in the lower range of power could be explained in Figure 7 as the engines starting to respond to the movement of power lever before achieving the go-around power lever angle. To match this behaviour, the delay δ of function (18) is set at a value of 2.75 seconds, accounting for 1 second advancement of power lever, 1 second for the engine to start responding, and 0.75 seconds assumed for the propeller adjustment delay.

In the report [14], it was mentioned that the aircraft stays at an altitude between 61 to 78 feet above ground level of 336 feet, or a minimum altitude of 397 feet above sea level. The altitude value from optimal control solution is lower

DOI: 10.13009/EUCASS2025-240

at 383 feet above sea level, or 47 feet above ground level. The higher value of FDR data could be attributed to the increase in lift generation capability of the wing in ground effect as the altitude is lower than the wing span, which was not considered in the methodology.

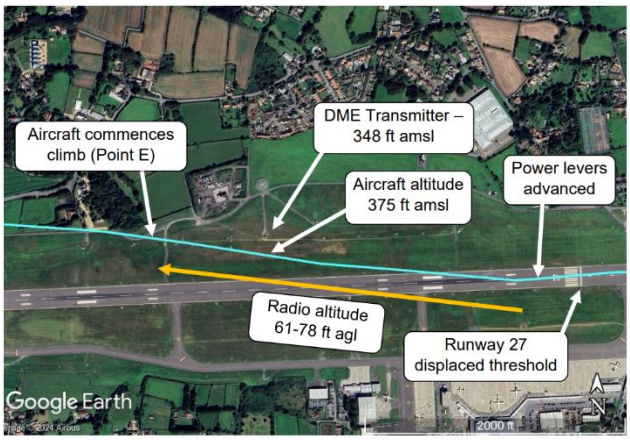

Figure 9: Ground track of reference data [13]

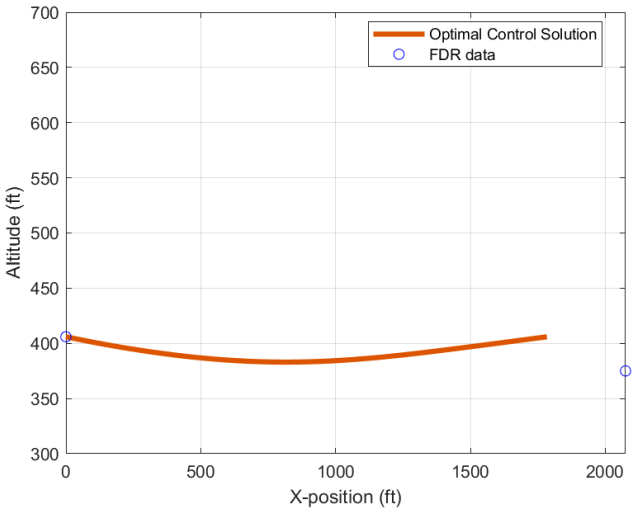

Figure 10: Altitude vs. x-position comparison

From the ground track of FDR data, although only a range of 61 – 78 ft is provided for the altitude, but at a distance of 2 075 ft from where the power levers are advanced, the aircraft achieves 375 ft altitude above mean sea level. However, the result of the optimal control method, shows that the aircraft has already regained the initial altitude at a distance of 1 783 ft. From the comparison of FDR data in Figure 7, this difference can be attributed to the different control strategy between optimal control solution and real flight data. In real operation, flight crew chose to increase the speed to around 130 knots by flying in a lower pitch angle, before pitching up for climb.

From the previous analysis, it can be concluded that the proposed optimal control strategy is able to replicate a realistic scenario with sufficient accuracy for the analysis of go-around manoeuvre with varying engine response time.

3.2 CS-25 OEI Go-around Case

Using the same methodology, an assessment to the go-around criteria stated in CS 25.101(g) [9] is performed. This case is relevant from an aircraft design perspective, as OEI engine climb gradient is one of the sizing criteria for the engine. Additionally, the determination of decision height based on the height loss during the manoeuvre, is an important consideration for maintaining operational safety.

Three examples have been worked out, each having different engine time constant $\boldsymbol{\tau}$ as described in Section 2.2. In these examples, the delay $\boldsymbol{\delta}$ of the engine is assumed to be 1 second to align with AMC25.101(g) [9].

The aircraft is considered to fly in a trimmed condition with an approach speed $\boldsymbol{V_0}$ of 96.1 knots, and a pitch angle $\boldsymbol{\gamma_0}$ of 7.9 degrees.

The resulting aircraft state history, as well as the control input history, is depicted in Figure 11 and Figure 12.

DOI: 10.13009/EUCASS2025-240

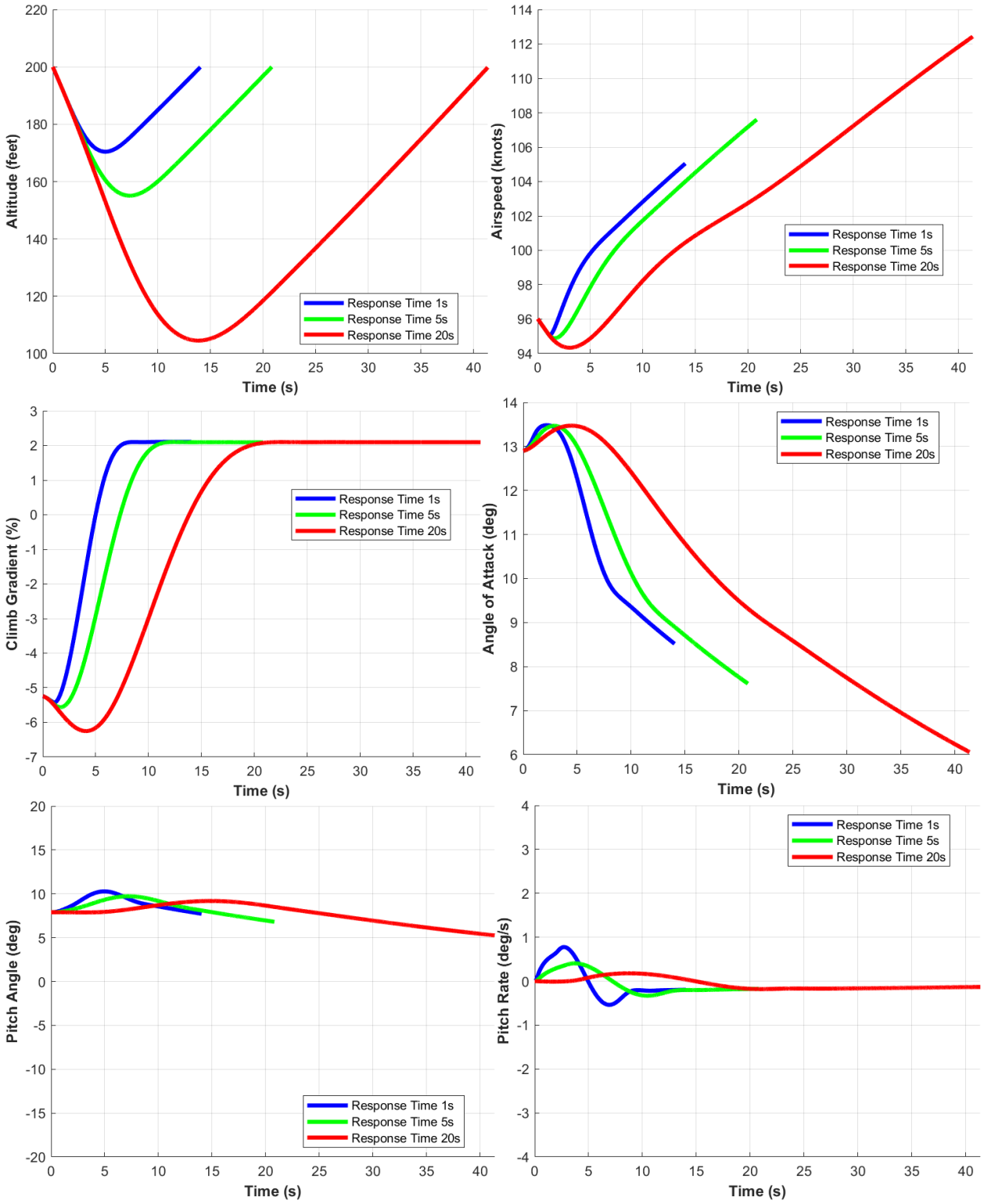

Figure 11: Time history of aircraft states for different engine response times in an OEI scenario: a) Altitude, b) Airspeed, c) Climb gradient, d) Angle of attack, e) Pitch angle, and f) Pitch rate

DOI: 10.13009/EUCASS2025-240

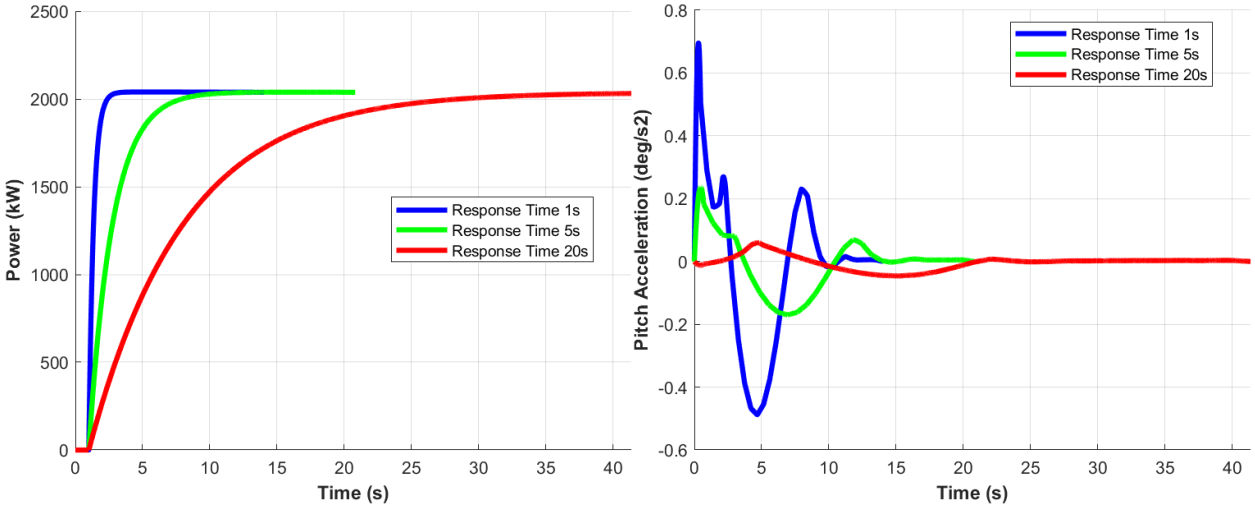

Figure 12: Time history of aircraft control: a) Power and b) Pitch acceleration

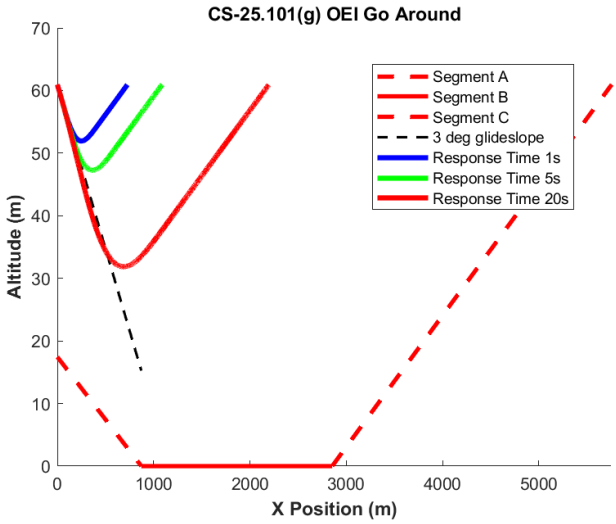

Figure 13: CS25.101(g) OEI go-around criteria comparison for different engine response times

Based on all of the figures in Figure 11, it can be seen that with increasing engine response times, the time needed to achieve a successful go-around is also increasing. The fastest engine achieved go-around within 14.0 seconds, followed by 20.8 seconds for the normal engine, and 41.3 seconds for the slowest engine.

The altitude behaviour as shown in Figure 11a with increasing response time also follows the same trend as time, with the minimum altitude reached during the go-around is decreasing or the altitude loss is increasing. The fastest engine experienced an altitude loss of 29 ft, followed by 45 ft for the normal engine, and 95 ft for the slowest engine.

The airspeed behaviour shown in Figure 11b is similar for all engines. All aircraft show a reduction of airspeed before going on an upward trend after reaching the lowest point. The time at this lowest point is different for each engine, where the fastest one reached a lowest airspeed of 95 knots in 1.1 seconds, the normal engine reached 94.9 knots in 1.6 seconds, and the slowest engine reached 94.3 knots in 3 seconds. These slightly different lowest airspeed values correlates with the engine response time, as a low speed means a lower drag for the aircraft to counteract and more thrust generated by the propeller.

In the angle of attack graph in Figure 11d, it is shown that the all engines required the same peak value, while the time of the peaks are different. The peak angle of attack is achieved at a time of 2.2 seconds, 2.8 seconds, and 4.6 seconds for the fast, normal, and slow engine case, respectively. This can be explained as the aircraft maximising the slope of the flight path angle, therefore the climb gradient, to achieve the go-around exit criteria as fast as possible.

From the graphs, it can also be seen that the pitch rate and pitch angle of all aircraft does not violate the limits to mitigate the risk of somatogravic illusion experienced by the flight crews, as shown in Figure 11f and Figure 11e.

DOI: 10.13009/EUCASS2025-240

The control input behaves similarly compared to each other; however, an interesting point in Figure 12b is that the optimal control input for aircraft with slower engine response have shallower slope and lower peaks. It must be pointed out that this particular optimal control solution is solving for a trajectory that minimizes the time needed for a go-around, setting the optimal control problem to minimize the altitude loss, or other criteria of concern, may yield different results.

This finding is counterintuitive to the aural terrain warning. It also supports the argument that pitching the aircraft nose up as fast as possible in event of an engine failure or deterioration in engine performance at low altitude is not the ideal course of action, therefore highlighting the importance of pilot training in emergency conditions.

Overall, comparing to the OEI go-around requirements of CS25.101(g) [9], all aircraft successfully performed a go-around manoeuvre with the optimal control input strategy. In this particular aircraft, the length of segment B of the OEI go-around criteria is not limiting the control strategy. However, this can be a different case if a larger aircraft with a higher approach speed is analysed. The height loss during the manoeuvre of an aircraft with a 20 seconds engine response time is 111% more than the 5 seconds response time engine, leaving much less margin of altitude for flight crew to work with, if the decision height remains the same. This result indicates that decision height must be considered consciously for novel engine architectures, with different response times.

4. Conclusion and Future Work

In this research, a methodology to assess the performance of an aircraft in a transient situation such as the go-around is presented. The methodology takes into account engine delay along with response time, which is not typically considered early in the conceptual design process, to consider a slower propulsion system such as SOFC-GT. However, the potential application of this method is not limited to a certain engine architecture, as the delays and time constant are also applicable to battery electric or any kind of propulsion system. The result shows that engine response and delay play a significant role in the performance of the aircraft in a transient situation.

A counterintuitive finding is that with a longer engine response time, the optimal strategy to perform a successful go-around that minimizes the time needed, is not to move the control surface slower compared to a faster engine. Results show a difference of up to 111% increased loss of altitude moving from 5 to 20 seconds response time. Hence, pilot training as well as supporting equipment that helps pilot to perform this kind of manoeuvre in emergency situations is crucial for the safety of flight.

This methodology has not yet taken into account the ground effect which will be the low-hanging fruit for future improvements, as well as integration of this methodology to a conceptual aircraft design loop, to see the effect of varying wing and flap dimensions to the transient performance.

Modelling the aircraft as a 1D beam instead of point mass can be explored. This should couple the pitch rate limit with the inertia of the aircraft with a relatively simple CG location shift that is expected of a hydrogen aircraft with an aft tank configuration. The beam model will also introduce balance of moments and a strategy of when to retract the flap during a go-around could be explored, providing more insight to the procedure of a go-around for aircraft with a slower engine response time.

A better engine model that captures the transient behaviour as well as emissions will also provide a more accurate picture of the transient performance of the aircraft, with a potential exploration into the trade-off between emissions and response time.

Acknowledgements

The research presented in this publication was partially performed under the HYLENA project. This project received funding from the European Union's Horizon Europe program for research and innovation under grant agreement No. 101137583. Additionally, we would like to thank Prof. Arvind Gangoli Rao and Dr. Feijia Yin for their input related to engine model and Dr. Carmine Varialle for his input on the formulation of optimal control problems.

DOI: 10.13009/EUCASS2025-240

References

[1] de Vries, Reynard, Hoogreef, Maurice F. M. and Vos, Roelof. 2020. Range Equation for Hybrid-Electric Aircraft with Constant Power Split. In : *American Institute of Aeronautics and Astronautics (AIAA), Journal of Aircraft, Vol. 57*, 552–557.

[2] Airbus. HYLENA - Hydrogen eLectrical Engine Novel Architecture. Airbus Research. https://research.airbus.com/en/products-systems/hylena.

[3] Filippone, A, and Mohammed-Kassim, Z. 2012. Multi-disciplinary Simulation of propeller-turboprop aircraft flight. In: *The Aeronautical Journal Vol. 116*, 985 - 1014

[4] Zhang, Biao, and al. 2022. Rapid load transition for integrated solid oxide fuel cell – Gas turbine (SOFC-GT) energy systems: A demonstration of the potential for grid response. In: *Energy Conversion and Management, Vol. 258*. 115544. ISSN: 0196-8904.

[5] EASA. 2023. CS-E Amendment 7.

[6] Kasmi, Hasnae, and al. 2023. Holistic Approach for Aircraft Trajectory Optimization Using Optimal Control. In: *American Institute of Aeronautics and Astronautics (AIAA), Journal of Aircraft, Vol. 60*. 1302–1313. ISSN: 1533-3868.

[7] Nie, Yuanbo, Faqir, Omar and Kerrigan, Eric C. 2018. ICLOCS2: Try this Optimal Control Problem Solver Before you Try the Rest. In: *12th International Conference on Control (CONTROL) Sheffield, UK, 5-7 Sept 2018*.

[8] Buell, Glenn and Leondes, C. T. 1973. Optimal Aircraft Go - Around and Flare Maneuvers. In: *IEEE Transactions on Aerospace and Electronic Systems*, 1973, Vol. AES 9

[9] EASA. 2023. Easy Access Rules for Large Aeroplanes (CS-25) (Amendment 27).

[10] Gudmundsson, Snorri. 2014. General Aviation Aircraft Design. General Aviation Aircraft Design. 342-365

[11] Drela, Mark. 1989. XFOIL: An Analysis and Design System for Low Reynolds Number Airfoils. 978-3-540-51884-6.

[12] Torenbeek, Egbert. 1989. Synthesis of Subsonic Airplane Design. 90-247-2724-3.

[13] Janes Information Group. 2009. Jane's All the World's Aircraft 2009–2010.

[14] AAIB Field Investigation. 2025. AAIB Report: ATR 72-500 (72-212A), LY-JUP. *Air Accidents Investigation Branch.* https://www.gov.uk/government/news/aaib-report-atr-72-500-72-212a-ly-jup